horticulturae

MDPI

Article

Autonomous UV-C Treatment and Hyperspectral Monitoring: Advanced Approaches for the Management of Dollar Spot in Turfgrass

Lorenzo Pippi [1,2], Lorenzo Gagliardi [1,*], Lisa Caturegli [1], Lorenzo Cotrozzi [1], Sofia Matilde Luglio [1], Simone Magni [1], Elisa Pellegrini [1], Claudia Pisuttu [1], Michele Raffaelli [1], Marco Santin [1], Marco Fontanelli [1], Tommaso Federighi [1], Claudio Scarpelli [3], Marco Volterrani [1] and Luca Incrocci [1]

[1] Department of Agriculture, Food and Environment (DAFE), University of Pisa, Via del Borghetto 80, 56124 Pisa, Italy; lorenzo.pippi@phd.unipi.it (L.P.); lisa.caturegli@unipi.it (L.C.); lorenzo.cotrozzi@unipi.it (L.C.); sofiamatilde.luglio@phd.unipi.it (S.M.L.); simone.magni@unipi.it (S.M.); elisa.pellegrini@unipi.it (E.P.); claudia.pisuttu@unipi.it (C.P.); michele.raffaelli@unipi.it (M.R.); marco.santin@unipi.it (M.S.); marco.fontanelli@unipi.it (M.F.); t.federighi@studenti.unipi.it (T.F.); marco.volterrani@unipi.it (M.V.); luca.incrocci@unipi.it (L.I.)

[2] University School for Advanced Studies IUSS Pavia, Piazza della Vittoria 15, 27100 Pavia, Italy

[3] Department of Energy, System, Territory and Construction Engineering (DESTeC), University of Pisa, Largo Lazzarino, 56122 Pisa, Italy; claudio.scarpelli@unipi.it

* Correspondence: lorenzo.gagliardi@agr.unipi.it

Abstract

Dollar spot is a severe and widespread turfgrass disease. Ultraviolet-C (UV-C) light treatment offers a promising management strategy, and its integration into autonomous mowers could reduce fungicide use, promoting sustainable and efficient turfgrass management. To ensure effectiveness and optimize intervention timing, monitoring is essential and hyperspectral sensing could represent a valuable resource. This study aimed to develop an innovative approach for the early detection and integrated management of dollar spot in bermudagrass by evaluating (i) the efficacy of an autonomous mower equipped with UV-C lamps in mitigating infections, and (ii) the potential of full-range hyperspectral sensing (350–2500 nm) for disease detection and monitoring. The autonomous mower enabled UV-C treatment with a field capacity of 0.04 ha h^{-1}, requiring 1.3 machines to treat 1 ha day^{-1}, and a primary energy consumption of 55.06 kWh ha^{-1} for a complete weekly treatment. Full-range canopy hyperspectral data (400–2400 nm) enabled rapid, non-destructive field detection. Permutational multivariate analysis of variance (PERMANOVA) detected significant effects of *Clarireedia jacksonii* (*Cj*; dollar spot pathogen) and the *Cj* × UV-C interaction. Partial least-squares discriminant analysis (PLS-DA) separated *Cj*+/UV+ and *Cj*+/UV− plots (Accuracy validation ≈ 0.73; $K \approx 0.69$). Investigated spectral indices confirmed *Cj* × UV-C interactions. Future research should explore how to optimize UV-C application regimes, improve system scalability, and enhance the robustness of hyperspectral models across diverse turfgrass genotypes, growth stages, and environmental conditions.

Keywords: integrated pest management; physical disease control; ultraviolet radiation; early disease detection; autonomous mowers; bermudagrass; spectral indices; vegetation spectroscopy

check for updates

Academic Editor: Stefano Marino

Received: 17 September 2025
Revised: 9 October 2025
Accepted: 14 October 2025
Published: 17 October 2025

Citation: Pippi, L.; Gagliardi, L.; Caturegli, L.; Cotrozzi, L.; Luglio, S.M.; Magni, S.; Pellegrini, E.; Pisuttu, C.; Raffaelli, M.; Santin, M.; et al. Autonomous UV-C Treatment and Hyperspectral Monitoring: Advanced Approaches for the Management of Dollar Spot in Turfgrass. *Horticulturae* **2025**, *11*, 1257. https://doi.org/10.3390/horticulturae11101257

Copyright: © 2025 by the authors. Licensee MDPI, Basel, Switzerland. This article is an open access article distributed under the terms and conditions of the Creative Commons Attribution (CC BY) license (https://creativecommons.org/licenses/by/4.0/).

1. Introduction

Dollar spot is a major and globally prevalent turfgrass disease affecting both warm- (C4) and cool-season (C3) species [1,2]. It is widespread across managed turfgrass systems such as golf courses, sport fields, and public and private gardens [3]. The causal agent, originally identified as the ascomycete *Sclerotinia homoeocarpa,* has since been reclassified into the genus *Clarireedia* with *C. jacksonii* (*Cj*) recognized as the most common species involved [4]. Symptoms, which include circular, straw-colored lesions often ranging in size to that of a silver dollar—hence the name dollar spot—vary depending on turfgrass species and management practices [5–7] and are favored by prolonged leaf wetness and high humidity. Control of dollar spot remains challenging and economically demanding [8,9], often requiring integrated strategies involving cultural practices, resistant cultivars, and repeated fungicide applications [10,11]. However, overreliance on chemical control has led to fungicide resistance and is increasingly restricted by regulatory policies, particularly in Europe [12–14]. In this context, advanced technologies such as optical sensors and precision turfgrass management offer promising tools for early detection, targeted intervention, and more sustainable disease control, helping to mitigate costs and reduce reliance on chemical inputs.

Ultraviolet-C (UV-C) radiation has emerged as a promising non-chemical strategy for managing fungal diseases in agriculture. While high doses can impair plant physiology by damaging DNA, proteins, and membranes, leading to reduced photosynthesis, growth, and vigor [15], low-dose applications have been shown to trigger plant defense responses [16–18] and simultaneously disrupt the cellular integrity of fungal pathogens [15]. Previous studies have reported that UV-C radiation can trigger plant defense mechanisms by stimulating the synthesis of secondary metabolites, enhancing antioxidant enzyme activities, and upregulating the expression of genes involved in the phenylpropanoid pathway [15,19,20]. Instead, the disruption of pathogen cellular integrity by UV-C radiation primarily occurs through DNA damage, resulting from the formation of pyrimidine dimers. The most effective range of the UV-C spectrum for inducing DNA damage lies between 254 and 262 nm [15,21]. Regarding experimental evidence, strawberries treated with UV-C radiation before harvest showed a lower incidence of spontaneous decay (39%) caused by *Botrytis cinerea* compared to untreated strawberries (76%) [16]. Similarly, Prämassing [22] investigates the effects of UV-C irradiations in *Clarireedia* infections in *Agrostis stolonifera* and *Poa annua*, reporting reduced disease coverage in plots treated with UV-C three times per week compared to untreated controls, with values of 0.75% and 2.5%, respectively.

Recent advances in agricultural robotics have enabled the integration of UV-C systems into autonomous platforms. For example, the Thorvald robot (Saga Robotics, Oslo, Norway) is a straddle-type machine developed for the management of fungal diseases such as powdery mildew in vineyards and strawberry crops [23]. Gadoury et al. [24] evaluated the application of UV-C light, delivered twice weekly at a dose of 200 J/m^2 using a straddle-type robot, in a Chardonnay vineyard, for the control of powdery mildew (*Erysiphe necator*). Authors observed a suppression of the pathogen on the fruit comparable to that achieved with a standard fungicide program (less than 5% of the cluster surface colonized), and significantly lower than in untreated controls (approximately 40%).

In turfgrass management, autonomous robotic mowers represent one of the earliest and most widespread applications of field robotics [25], offering sustainable, battery-powered maintenance for residential, urban, and sports landscapes [25,26]. Building on these innovations, UV-C-based systems for dollar spot control in turfgrass, such as the walk-behind UV-C180 (SGL, Waddinxveen, The Netherlands) [27] and the tractor-mounted Helios Gazon (UVBOOSTING, Saint-Nom-la-Bretèche, France) [28], have recently been developed. The UVBOOSTING technology, for example, has been developed based on the

effect of UV-C distribution in the form of flashes, which stimulates the plant's defensive response [29–31]. By pre-activating these mechanisms, plants become more resistant to damage caused by pathogens.

A key frontier now lies in integrating UV-C lamps into autonomous mowing robots, thus enabling both lawn maintenance and pathogen suppression. This dual-function approach has the potential to reduce fungicide use and support sustainable turfgrass management. However, to ensure effectiveness, such systems must be coupled with targeted, consistent monitoring strategies for early disease detection and optimized intervention timing.

Among the emerging tools to enhance turfgrass disease management, advanced phenotyping technologies, particularly vegetation spectroscopy, offer rapid, non-destructive insights into plant health. This high-throughput sensing method exploits the optical properties of leaf and canopy tissues to assess physiological status, enabling the simultaneous evaluation of multiple traits linked to stress responses [32,33]. Spectral data are obtained from variations in the vibrational excitation of molecular bonds (e.g., C–H, N–H, O–H) when exposed to specific wavelengths across the visible (VIS), near-infrared (NIR), and short-wave infrared (SWIR) regions [34]. Recent progress in portable spectrometers, data processing, and chemometric modeling has expanded the field applicability of hyperspectral reflectance. Applications include the use of vegetation spectral indices (e.g., NDVI, PRI) and the interpretation of spectral patterns as proxies for plant morphological, biochemical, and physiological responses under stress [35]. Additionally, vegetation spectroscopy can be scaled up via airborne or satellite imaging systems, enabling large-scale turfgrass monitoring. Despite its growing use in crop phenotyping, its application in turfgrass disease detection, especially for pathogens like *Clarireedia* spp., remains limited and underexplored, highlighting the need for further research in this field [36].

The aim of this study was to develop an innovative approach for the early detection and integrated management of dollar spot in bermudagrass (*Cynodon dactylon*), one of the most used warm-season turfgrasses in Italy. Following preliminary in vitro tests assessing the effects of UV-C radiation on *C. jacksonii* (*Cj*) [37], a field trial was conducted with two main objectives: (i) to evaluate the efficacy of autonomous mowers equipped with UV-C lamps in mitigating *Cj* infections, and (ii) to investigate the potential of full-range hyperspectral sensing (350–2500 nm) for the early detection and monitoring of the disease (i.e., index-based tracking of pathogen-induced reflectance responses from field spectroradiometer signatures). Specifically, our goal was to understand the overall UV-C effect on disease development, whether through limiting pathogen spread and/or activating plant defense responses. By combining high-resolution spectral diagnostics with an alternative, non-chemical treatment strategy, this study aims to contribute to more precise, sustainable, and technologically integrated turfgrass disease management, offering turfgrass managers and practitioners a versatile tool for reducing fungicide dependence while improving control effectiveness.

2. Materials and Methods

2.1. Implementation of an Autonomous Mower Equipped with UV-C Lamps

The autonomous mower used in this study was a two-wheel-drive prototype (1.20 × 1.15 × 0.48 m in length, width, and height). The machine features a cutting system composed of two disks, each with a cutting width of 0.40 m. Each disk is equipped with two thin, sharp blades. For power, the mower used a 36.3 V, 49.0 Ah lithium battery with an energy capacity of 1778.7 Wh. During the trial, the cutting system was not activated to limit the effects of external variables, and the battery was used exclusively to power the mower movement, which was operated via remote control. Additionally, the mower was

fitted with a coupling device that allowed the attachment to a UV-C lamp-carrying frame (Figure 1).

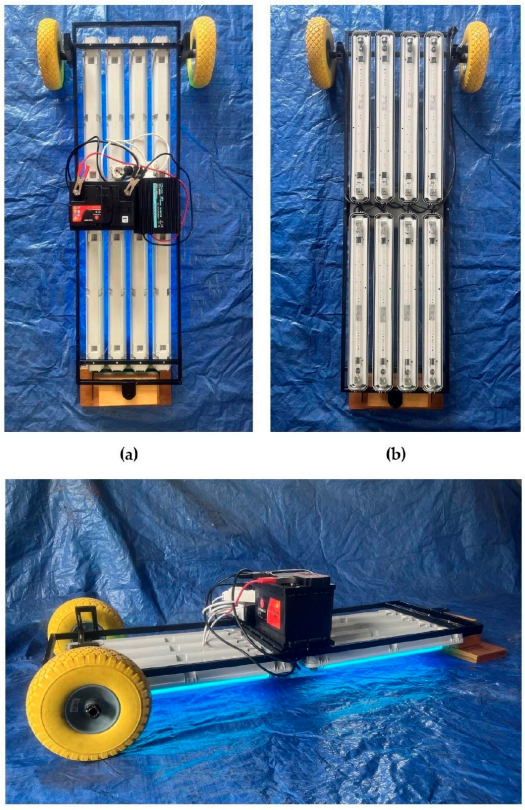

Figure 1. Frontal (**a**), ventral (**b**) and side view (**c**) of the UV-C lamp carrying frame employed in the trial.

The frame was designed to pivot freely at the attachment point, allowing it to follow the mower's movements and change direction accordingly. Constructed from iron profiles with a rectangular cross-section measuring 2 × 1.5 cm, the lamp-carrying frame was supported at the rear by freely rotating wheels with a diameter of 25 cm. It housed eight lamp fixtures, arranged with four positioned at the front and four at the rear. This configuration was selected to deliver a daily UV-C dose of 101.47 μJ cm^{-2}, as determined in preliminary laboratory tests [37]. The fixtures used were fluorescent lamp holders (921 Hydro T8 EL, Disano Illuminazione S.P.A., Rozzano, Italy) with a 230 V/50 Hz power supply and electronic ballast. Each fixture measured 69 cm in length and 9.2 cm in width, with a weight of 0.92 kg. They were equipped with UV-C fluorescent lamps (TUV T8 F17 1SL/25, Philips, Amsterdam, The Netherlands) that operated at 16.7 W, with a nominal current of 0.236 A and nominal voltage of 72 V. The lamps emitted UV-C radiation with a peak wavelength of 253.7 nm, which is optimal for germicidal activity. Each lamp measured 60.4 cm in length, 2.8 cm in diameter, and weighed 0.08 kg. To maximize UV-C exposure, the lamps were installed without protective shielding. The frame height was calibrated by adjusting the towing point and wheel attachments, ensuring that the lamps remained at a fixed distance of 5 cm above the turfgrass surface.

The frame also included a dedicated platform to carry a 12 V, 55 Ah lead-acid battery (13.1 kg) and an inverter. The inverter had an input voltage range of 10–15 V (DC), an output voltage of 230 V (AC), an output power of 600 W, and an efficiency of 90%. These components were essential for powering the UV-C lamps. Overall, the complete lamp system—

including the frame, light fixtures, lamps, battery platform and inverter—measured 140 cm in length, 43 cm in width, and had a total weight of 31.5 kg.

2.2. Field Trial

2.2.1. Plant and Fungal Material

The field trial was conducted in summer 2024 at the Centre for Research on Turfgrass for Environment and Sports—CeRTES, Department of Agriculture, Food and Environment, University of Pisa (San Piero a Grado, Pisa; 43°40′33″ N 10°18′41″ E, 2 m a.s.l.) on a mature stand of bermudagrass (*Cynodon dactylon* × *transvaalensis* "Patriot"). The soil was classified as silty loam (28:55:17% sand:silt:clay), with an organic matter content of 18 g kg^{-1}, and a pH of 7.8. A turfgrass scalping to a height of 1 cm was performed on 7 June. Fertilization was carried out on 11 June applying 168 kg ha^{-1} of nitrogen (Ubesol 45 granulare, Vialca Srl, Uzzano, Italy, 21–0–0).

An isolate of *Cj*, purchased from a fungal culture collection in Nothern Italy, was grown on Petri dishes (Ø 14 cm) containing Potato Dextrose Agar (PDA, 42 g L^{-1}, Biolife Italiana S.r.l., Milan, Italy) amended with streptomycin sulfate (0.1 g L^{-1}, Gold Biotechnology, Inc., St. Louis, MO, USA). Petri dishes were incubated for 7 days at 23 °C with a 12 h photoperiod. The artificial inoculum was prepared by suspending *Cj* mycelium in sterile water (100 g L^{-1}), incubated at 23 °C for 48 h in an orbital shaker at 150 rpm (711 CT®, Asal, Milan, Italy), before use [4].

2.2.2. Experimental Design

The field was divided into four experimental groups: (i) inoculated with *Cj* and treated with UV-C (*Cj*+/UV+); (ii) inoculated and not treated (*Cj*+/UV−); (iii) not inoculated and treated (*Cj*−/UV+); and (iv) not inoculated and not treated (*Cj*−/UV−; control). A randomized complete block design with three replicates (plots) was used. Each experimental plot measured 9 m in length and 0.43 m in width.

Clarireedia jacksonii inoculation was conducted on 3 July by spraying the mycelial suspension onto the selected turfgrass areas (*Cj*+). This was performed using a Nebla Electric backpack sprayer (Stocker Srl, Lana, Italy), equipped with a 15 L tank, Li-ion battery (18 V, 2.2 Ah), an FPM seal set, and a spray lance with nozzle. For each treatment, 0.5 L of mycelial suspension was applied, with the drip rate set at 0.1 L min^{-1}. One week later, the UV-C treatment began, using the autonomous mower equipped with the lamp system. The treatment was applied daily, for seven consecutive days, following the protocol established in previous laboratory trials by [37]. At the time the UV-C treatment started, the turfgrass had an average height of 5.5 cm. At the end of the trials, symptom development was assessed by considering the percentage of infected area of the total turf surface, as previously reported in Santin et al. [34] For this purpose, the whole inoculated turfgrass areas were divided in 0.5 m^2 sections and photographs were taken. Concomitantly, leaf samples were collected to check the presence of fungal propagules [37].

2.3. Data Collection

2.3.1. Operative Performance of the Autonomous Mower Equipped with the UV-C Lamp System

Parameters related to the operational performance of the autonomous mower equipped with UV-C lamps were evaluated. The travel time required to cover a straight-9 m section within the experimental area was recorded to calculate the working speed of the machine. Additionally, the time needed to perform turning maneuvers was measured. These parameters, along with the working width of the UV-C lamp frame, were used to estimate the total field operation time. Electrical energy consumption by both the mower and the UV-C lamps was measured using a power consumption meter (EL-EPM02HQ;

Nedis's-Hertogenbosch, The Netherlands). The energy autonomy of the system was calculated based on the assumption that the mower's battery simultaneously powered both the robot's movement and the UV-C lamps. From these data, the number of autonomous mowers equipped with the UV-C system required to treat one hectare per day was estimated. Primary energy consumption for completing a full one-week treatment cycle over one hectare was determined by factoring in the conversion efficiency of the Italian National Electric System (0.566) [38], the efficiency of lithium-ion batteries (91%) [39], and that of lead-acid batteries (85%) [40].

2.3.2. Collection of Canopy Spectra

Canopy reflectance profiles were acquired using an ASD FieldSpec® 4 High-Resolution spectroradiometer (Analytical Spectral Devices, Boulder, CO, USA), operating over the 350–2500 nm spectral range. The instrument was equipped with a pistol grip to facilitate consistent and accurate targeting of the turfgrass canopy. Canopy reflectance was measured between 11:00 a.m. and 1:00 p.m. under clear sky conditions, using a fiber-optic cable with an eight-degree field of view (covering approximately 12 cm^2 of surface), mounted on a pistol grip and positioned one meter above the canopy, with the sensor oriented nearly perpendicular to the turfgrass canopy surface. Reflectance was calculated by normalizing radiance values to those of a Spectralon® Diffuse Reflectance Target (Labsphere, Inc., North Sutton, NH, USA), with reference measurements collected after every nine canopy spectra to ensure accuracy. Each experimental plot was sampled at nine evenly distributed points, corresponding to one measurement per linear meter along the plot's length. At the time of spectral acquisition, all plots were visually asymptomatic. The disease's presence was subsequently confirmed at the end-of-trial assessment.

2.4. Analyses of Spectral Signatures

The effects of *Cj* infection, UV-C radiation treatment (UV-C), and their interaction on turfgrass canopy reflectance were assessed by Permutational Analysis of Variance (PERMANOVA) [41]. Spectral regions between 1350 and 1500 nm and 1750–2000 nm were excluded from the analysis due to strong atmospheric water absorption interference. Dissimilarity among spectral profiles was calculated using Euclidean distances, and 10,000 permutations were conducted to ensure robust statistical inference. To visualize differences in spectral patterns identified by PERMANOVA, Principal Coordinates Analysis (PCoA) was performed. This ordination technique reduces data dimensionality by computing uncorrelated axes (coordinates) from Euclidean distance matrix. Analyses were performed using the 'vegan' package in R (version 2024.12.0+467) [42]. To evaluate the discrimination accuracy of experimental groups by hyperspectral data, Partial Least Squares Discriminant Analysis (PLS-DA) was applied [43]. To ensure robust model evaluation, PLS-DA was repeated 500 times, with datasets randomly split into calibration (training) and validation (testing) subsets. Model performance was assessed based on classification accuracy for both subsets. Various calibration-to-validation ratios (50:50, 70:30, and 80:20) and different numbers of latent variables were tested to identify the optimal model configuration. The kappa statistic was used as the primary metric to select the most accurate and reliable models. PLS-DA implementation was carried out using the 'caret' and 'vegan' packages in R [42,44].

2.5. Calculation of Vegetation Spectral Indices

Seven largely used vegetation spectral indices were calculated: Normalized Difference Vegetation Index [NDVI = $(R_{780} - R_{570})/(R_{780} + R_{570})$; [45]]; Normalized Difference Water Index [NDWI = $(R_{857} - R_{1241})/(R_{857} + R_{1241})$; [46]]; Chlorophyll Index [CI = $(R_{750} - R_{705})/(R_{750} + R_{705})$; [47]]; Carotenoid Reflectance Index [CRI = $(R_{510})^{-1} - (R_{550})^{-1}$; [48]];

Anthocyanin Reflectance Index [ARI = $(R_{550})^{-1} - (R_{700})^{-1}$; [49]]; Plant Senescence Reflectance Index [PSRI = $(R_{678} - R_{500})/R_{750}$; [50]]; and Normalized Difference Lignin Index [NDLI = $[\log(1/R_{1754}) - \log(1/R_{1680})]/[\log(1/R_{1754}) + \log(1/R_{1680})$; [51]]. R_x means reflectance at x nm wavelength. The seven indices were selected to reflect turfgrass-dollar spot pathophysiology and the operational aim of preserving canopy greenness under pre-visual conditions: greenness/chlorophyll (NDVI, CI), stress-pigment and senescence signals (ARI, CRI, PSRI), water status (NDWI), and structural/nitrogen proxies (NDLI, NDNI).

2.6. Statistical Analysis

The Shapiro–Wilk test was initially employed to evaluate the normality of the distribution of calculated vegetation spectral indices. Subsequently, a two-way analysis of variance (ANOVA) was performed to evaluate the effects of fungal infection (*Cj*), UV-C treatment (UV-C), and their interaction on vegetation spectral indices. When significant effects were detected ($p \leq 0.05$), mean differences were evaluated using Tukey's honestly significant difference test. All analyses were carried out using JMP Pro 13 software (SAS Institute Inc., Cary, NC, USA).

3. Results

3.1. Operative Performance of the Autonomous Mower Equipped with UV-C Lamp System

To ensure the delivery of the appropriate UV-C dosage, the machine operated at a reduced working speed of 0.95 km·h^{-1}, resulting in a limited working capacity of 0.04 ha·h^{-1}.

The energy required for the propulsion of the autonomous mower and the operation of the UV-C lamps amounts to 0.161 kWh·h^{-1}. With a UV-C irradiation time per system charging cycle of 10.6 h and a battery recharging time per cycle of 2.5 h, the total UV-C irradiation time per day is 19.4 h, with a daily charging time of 4.58 h, resulting in a daily energy consumption of 3.13 kWh. Considering the working capacity of a single autonomous mower equipped with a UV-C lamp system, 1.3 machines are required to treat 1 hectare of turfgrass in one day, with a daily energy consumption of 4.05 kWh, and a primary energy consumption of 7.87 kWh. Completing a full treatment cycle, lasting one week, on a 1-hectare area results in a total energy consumption of 28.36 kWh, and a primary energy consumption of 55.06 kWh.

3.2. Analysis of Canopy Hyperspectral Signatures

At the end of the trials, no symptoms appeared in inoculated and/or UV-C treated turfgrass, even if fungal propagules were successfully isolated from infected leaves. Various spectral ranges were explored to achieve the best PERMANOVA statistical performance for canopy hyperspectral signatures of bermudagrass, and the best results were obtained using all the available wavelengths (i.e., 400–2400 nm) excluding the 1350–1500 and 1750–2000 nm regions affected by atmospheric water absorption (Figure 2). Figure 2A summarizes spectral variability, Figure 2B shows the treatments' mean spectra and Figure 2C reports the percentage differences relative to the *Cj*−/UV− conditions. PERMANOVA revealed significant effects for *Cj* and UV-C light treatment, as well as their interaction (Table 1). The best classification of the experimental groups (i.e., higher mean kappa) by PLS-DA of hyperspectral data was determined with an 80:20 calibration-to-validation data ratio, using 33 components. The validation accuracy and kappa were 0.73 ± 0.12 and 0.69 ± 0.16, respectively (mean ± standard deviation; Figure 3). Table 2 reports on the confusion matrix detailing classification accuracy among experimental groups. The best classification performance was achieved under *Cj*+/UV+ conditions, with an accuracy of 0.84. Plants that were only inoculated (*Cj*+/UV−) were classified with an accuracy of 0.74, while the non-inoculated plants, either not exposed (*Cj*−/UV−) or exposed (*Cj*−/UV+) to UV-C were

distinguished with an accuracy of 0.64 and 0.66, respectively. Because all canopy spectra were collected from visually asymptomatic plots, the discrimination among management conditions indicates pre-visual spectral separation.

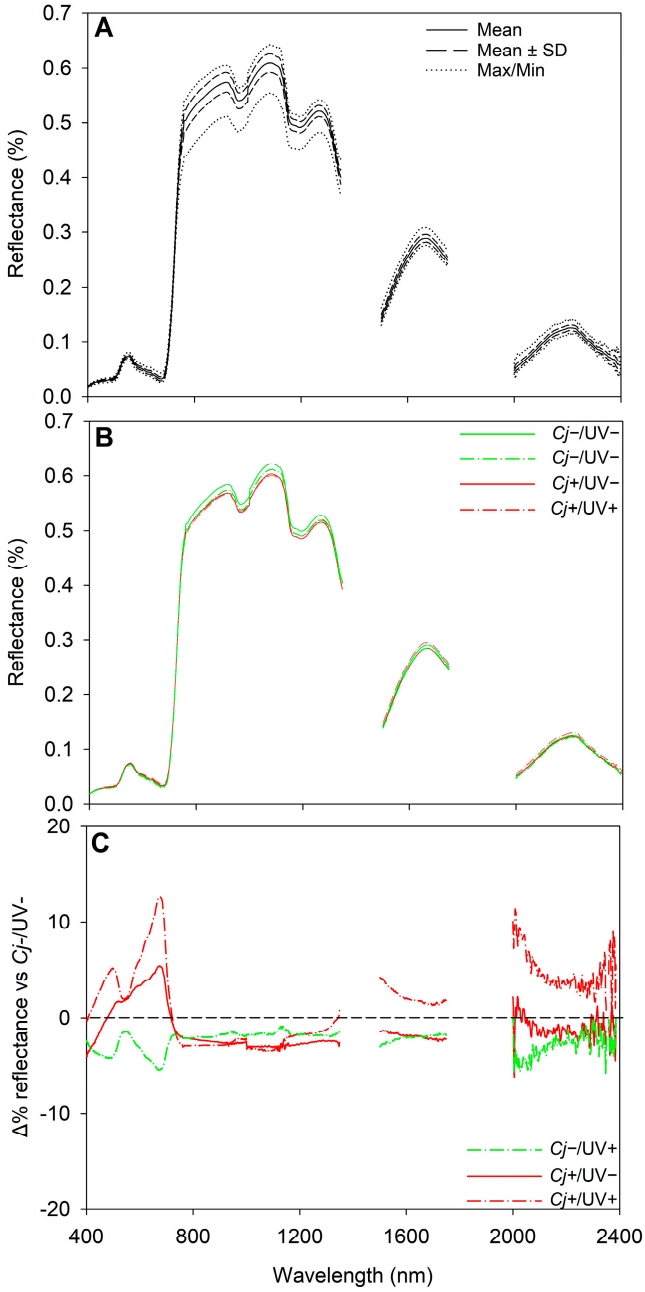

Figure 2. Canopy hyperspectral measurements repeatedly collected in bermudagrass inoculated with *Clarireedia jacksonii* and exposed to UV-C light treatment. (**A**) Distribution of all spectra across the study: mean (solid line), mean ± standard deviation (dashed), minimum and maximum (dotted). (**B**) Group means by treatment: uninoculated (green) vs. inoculated (red), each under no UV-C (solid) or UV-C (dash-dot): *Cj*-/UV−, *Cj*−/UV+, *Cj*+/UV−, *Cj*+/UV+. (**C**) Percentage difference in reflectance relative to the uninoculated, no-UV control (*Cj*−/UV−), computed as $\Delta\% = [(R_T) - (R_C)/(R_C)] \times 100$, R_C indicates reflectance of plants under 'control' conditions. Curves show treatment means; the dashed horizontal line indicates parity (0%).

Table 1. *p* levels of two-way permutational multivariate analysis of variance (PERMANOVA) for the effects of *Clarireedia jacksonii* (*Cj*) infection, UV-C treatment and their interaction on the full-range (400–2400 nm) reflectance profiles collected at canopy-level from *Cynodon dactylon* turfgrass. *df* represents the degrees of freedom. *** $p \leq 0.001$, ** $p \leq 0.01$, ns $p > 0.05$.

Effect	*df*	*p*
Cj	1	***
UV-C	1	ns
Cj × UV-C	1	**

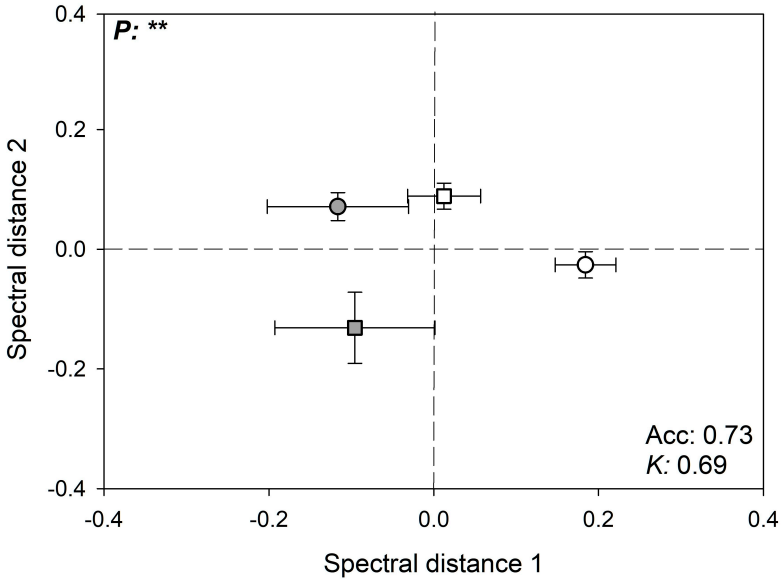

Figure 3. Scores (mean ± standard error) of the first and second principal components from a principal coordinates analysis of canopy reflectance data (400–2400 nm) collected from *Cynodon dactylon* under different treatments: not inoculated and untreated (*Cj*−/UV−; white circle), inoculated with *Clarireedia jacksonii* (*Cj*+/UV−; gray circle), irradiated with UV-C (*Cj*−/UV+; white square), inoculated with *C. jacksonii* and irradiated with UV-C (*Cj*+/UV+; gray square). The accuracy and kappa values generated via partial least square discriminant analysis and the *p* value are reported; ** $p \leq 0.01$.

Table 2. Confusion matrix from PLS-DA for the accuracy of discrimination for single levels of *Clarireedia jacksonii* infection (*Cj*) and UV-C light treatment (UV-C) interaction (*Cj* × UV-C) using 33 components. *Cj*−/UV− means not inoculated and not UV-C treated plants, *Cj*+/UV− means inoculated and not UV-C treated plants, *Cj*−/UV+ means not inoculated and UV-C treated plants, *Cj*+/UV+ means inoculated, and UV-C treated plants. Bold values correspond to the correct classification rates (per-class accuracy) for the respective group, calculated as the proportion of spectra correctly identified by the model.

Experimental Groups	C−/U−	*Cj*+/UV−	*Cj*−/UV+	*Cj*+/UV+
Cj−/UV−	0.66	0.08	0.24	0.02
Cj+/UV−	0.09	0.76	0.09	0.06
Cj−/UV+	0.16	0.20	0.64	0.00
Cj+/UV+	0.08	0.09	0.00	0.83

3.3. Variations in Vegetation Spectral Indices

The effects of *Cj* infection, UV-C treatment, and their interaction are reported in Table 3. The *Cj*+/UV+ effect was significant for all the calculated vegetation spectral indices, except for NDVI, NDNI and CRI, for which however we observed a significant

Cj effect, as they decreased by 1.27%, 2.23%, and 2.60% due to inoculation (compared to plants not inoculated, as average). CI decreased by 3.59% in *Cj*+/UV+ plants, compared to controls (i.e., *Cj*−/UV−; Figure 4c), while ARI and PSRI increased by 114,08% and 0.53%, respectively (Figure 4d,e). *Cj*+/UV+ plants also showed lower NDWI values than *Cj*−/UV+ ones (Figure 4b), while NDWI was 14.53% lower in *Cj*+/UV− compared to controls (Figure 4a).

Table 3. F value and *p* levels of two-way repeated measures analysis of variance (ANOVA) for the effects of *Clarireedia jacksonii* infection (*Cj*), UV-C light treatment (UV-C) and their interaction on vegetation spectral indices calculated from *Cynodon dactylon* canopy. *df* represents degrees of freedom (***: $p \leq 0.001$, **: $p \leq 0.01$, *: $p \leq 0.05$, ns; $p > 0.05$). Abbreviations: NDVI, normalized difference vegetation index; NDLI, normalized difference lignin index; NDNI, normalized difference nitrogen index; CI, chlorophyll index; CRI, carotenoid reflectance index; NDWI, normalized difference water index; PSRI, plant senescence reflectance index; ARI, anthocyanins reflectance index.

Index	*Cj* (*df*: 1)	UV-C (*df*: 1)	*Cj* × UV-C (*df*: 1)
NDVI	8.37 **	0.44 ns	0.26 ns
NDLI	0.21 ns	2.96 ns	5.06 **
NDWI	0.40 ns	3.94 ns	6.02 **
CI	9.80 **	2.81 ns	4.86 **
ARI	21.78 ***	6.21 *	24.51 ***
PSRI	22.47 ***	1.78 ns	44.60 **
NDNI	14.53 ***	1.26 ns	0.53 ns
CRI	4.43 *	0.10 ns	2.48 ns

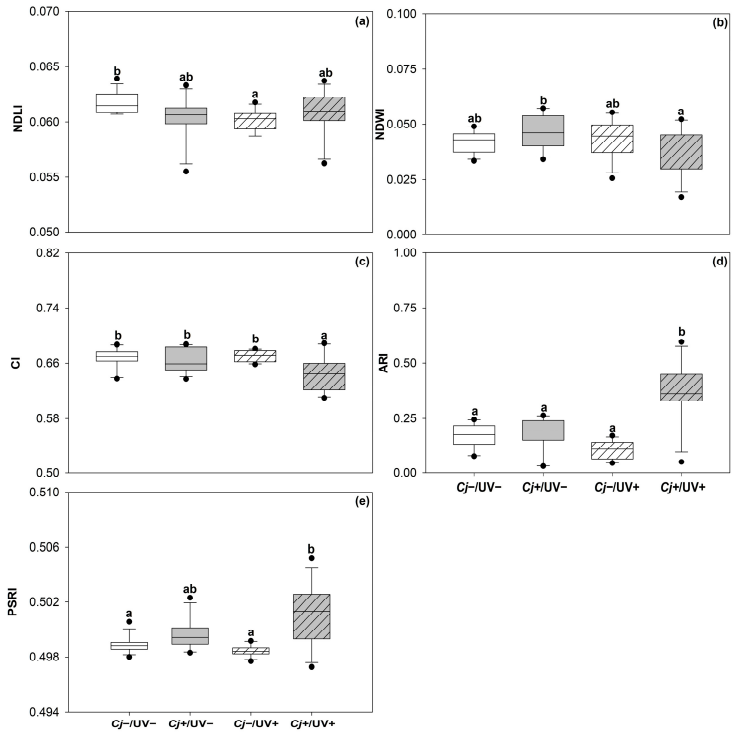

Figure 4. Values of normalized difference lignin index (NDLI) (**a**); normalized difference water index (NDWI) (**b**); chlorophyll index (CI) (**c**); anthocyanin reflectance index (ARI) (**d**) and plant senescence reflectance index (PSRI) (**e**) estimated from *Cynodon dactylon* canopy spectra under different *Clarireedia jacksonii* (*Cj*) and UV-C light treatment (UV-C) conditions. Different lowercase letters indicate statistically significant differences ($p \leq 0.05$). *Cj*−/UV− means not inoculated and not UV-C treated plants, *Cj*+/UV− means inoculated and not UV-C treated plants, *Cj*−/UV+ means not inoculated and UV-C treated plants, *Cj*+/UV+ means inoculated, and UV-C treated plants.

4. Discussion

Turfgrass systems are essential to various managed landscapes, such as golf courses, sports fields, and amenity lawns, where consistent quality, playability, and resilience to biotic stressors are critical for performance and esthetics. Improving the sustainability of turfgrass disease management, particularly for common fungal pathogens like *Cj*, the causal agent of dollar spot, is critical for maximizing ecosystem services and reducing environmental disservices [52]. This study highlighted the potential of two approaches for turfgrass management: automatized UV-C-based disease suppression and hyperspectral phenotyping for disease detection. The results demonstrate the potential of both technologies to enhance disease control efficacy and monitoring precision while promoting environmentally responsible practices.

UV-C radiation has emerged as a promising non-chemical alternative for managing plant diseases, having been shown to effectively suppress the growth and proliferation of a range of fungal pathogens. Studies have demonstrated its efficacy against powdery mildew on strawberry (caused by *Podosphaera aphanis)* [53], *Botrytis cinerea* (gray mold on strawberry), and *Monilinia fructigena* (brown rot on strawberry and cherry) [54–56], highlighting its potential for broad-spectrum disease control. To the best of our knowledge, this study is among the first to evaluate UV-C-based management of dollar spot in turfgrass using an autonomous robotic platform. A previous work by Prämassing [22] investigated the impact of UV-C treatment on *Clarireedia* infections in *Agrostis stolonifera* and *Poa annua*, showing that repeated exposure to UV-C doses of 35–40 mJ cm^{-2}, applied three times per week, significantly reduced disease coverage to 0.75% and 2.5%, respectively, compared to untreated controls.

The use of the autonomous mower equipped with a UV-C lamp system enabled the application of turfgrass treatment at the dosage considered most appropriate. Based on our estimates, the primary energy consumption for a complete weekly treatment on 1 ha is approximately 55.06 kWh ha^{-1}. As highlighted by Scolaro et al. [57], electric machines offer significant benefits compared to those powered by internal combustion or hybrid (diesel-electric) engines, including lower primary energy consumption and reduced on-site carbon dioxide emissions, thus promoting more sustainable agricultural practices. Additionally, the combination of a lightweight UV-C lamp system with a compact autonomous mower—compared to larger turfgrass management equipment such as utility golf carts, tractors, and ride-on mowers- helps minimize soil compaction issues [58]. However, the system also presents logistical challenges. The required low forward speed of 0.95 km h^{-1} to deliver the correct UV-C dosage resulted in a limited field capacity of 0.04 ha h^{-1}, necessitating more than one machine to cover 1 ha per day. This could lead to management disadvantages due to the increased time required for installing charging bases, as well as for machine management and maintenance [59]. Improving the irradiance of UV-C lamps would be crucial for improving management efficiency, potentially reducing treatment time, and enabling higher working speeds. However, it is important to note that delivering the same dosage at higher irradiance over shorter periods could not produce equivalent effects to lower irradiance over longer periods [31]. Interestingly, recent studies suggest that brief UV-C flashes (typically under 2 s) at hormetic doses (e.g., 1 kJ m^{-2} for lettuce, tomato, and grapevine, and up to 1.70 kJ m^{-2} for strawberry) may represent optimized treatments to stimulate plant resilience [29,31,55,60]. These ultra-short exposures have been shown to be more effective than conventional longer illuminations (60 s or more) in stimulating plant defenses, possibly due to differential activation of perception and signaling pathways [29,31]. Future research should therefore optimize UV-C delivery regimes to balance treatment efficacy, plant tolerance, and operational feasibility, with

particular attention to flash-based protocols that may enhance such beneficial effects while minimizing potential photodamage.

In parallel, our study showed that full-range canopy hyperspectral data (400–2400 nm) provide a rapid, non-destructive method for detecting dollar spot under field conditions. This aligns with growing interest in using advanced sensing for turfgrass research and precision management. Previous studies have applied spectral data to assess abiotic stressors such as drought and nitrogen deficiency [61] or to discriminate between turfgrass species and cultivars with high accuracy [62]. Although most dollar spot detection efforts to date have relied on RGB image-based machine learning approaches [63], our results show that hyperspectral phenotyping can identify the pathogen even before visible symptoms appear. Using PLS-DA, we were able to distinguish experimental groups (i.e., *Cj* infection and UV-C treatment combinations) with high classification accuracy (73%, as average), demonstrating the feasibility of early disease diagnosis. The PLS-DA achieved its best classification performance under *Cj*+/UV+ conditions (accuracy = 0.84). Distinguishing between plants only exposed to UV-C (*Cj*−/UV− and *Cj*−/UV+) proved more challenging with an accuracy of 0.66 and 0.64, respectively. An accuracy of 0.74 was obtained for *Cj*+/UV−, indicating a good ability of the PLS-DA classification to detect pathogen-inoculated plants in the absence of UV-C treatment.

This capability addresses key limitations of traditional visual assessment methods, which are inherently subjective and evaluator-dependent [64].

Variations in vegetation spectral indices provided further insight into plant physiological responses to *Cj* infection and UV-C treatment. Several indices, i.e., NDLI, NDWI, CI, ARI, and PSRI, showed significant interactions between pathogen presence and UV-C treatment, indicating that these combined stressors induce measurable changes in turfgrass spectral signatures. These spectral changes likely reflect the metabolic reprogramming triggered by hormetic UV-C doses, which have been shown to stimulate the accumulation of defense-related secondary metabolites including phenolic compounds, flavonoids, anthocyanins, and phytoalexins across diverse plant species [29,65,66]. NDLI, which is associated with lignin and structural cell wall components [51], increased under *Cj*+/UV+ treatment. This may reflect an induced reinforcement of cell walls, consistent with previous reports of UV-C stimulating secondary metabolite synthesis and enhancing pathogen resistance [15]. NDWI decreased in plots subjected to *Cj*+/UV+, suggesting changes in water retention or cuticle integrity. Prior work [16,17] indicates that UV-C may prime plant defenses by altering transpiration rates and enhancing cuticle thickness, which could modify water-related reflectance properties. Hormetic UV-C treatments, particularly when delivered as brief flashes, have been demonstrated to induce structural modifications at the leaf surface, including stomatal occlusion by wax-like matrices and cuticle reinforcement, which enhance pathogen resistance while maintaining normal physiological function [67,68]. Moreover, UV-C priming has been shown to activate systemic defense pathways without metabolic impairments under non-stress conditions, as evidenced by unchanged growth parameters and metabolome profiles in treated plants [68]. CI, ARI and PSRI showed coordinate and directionally consistent response under *Cj*+/UV+ condition. Specifically, CI declined exclusively under *Cj*+/UV+, potentially reflecting a shift in resource allocation from photosynthesis toward defense metabolite production. This is consistent with the known tradeoff between chlorophyll biosynthesis and defense activation during systemic acquired resistance [17]. In contrast, PSRI peaked under *Cj*+/UV+ condition. This index, sensitive to chlorophyll/carotenoid ratio, often increases during stress-induced senescence or pigment restructuring [50]. The elevated PSRI may signal a local senescence response and an upregulation of carotenoids for photoprotection under mild UV-C exposure. Similarly, ARI was highest in *Cj*+/UV+ plants reflecting anthocyanin accumulation, known

to be triggered by both UV-C and pathogen stress, which serves antioxidant and structural defense roles [16,48]. The synchronous divergence of these three indices, especially under *Cj*+/UV+, underscores a concerted shift in pigment-related processes. Moreover, NDVI, NDNI and CRI were significantly affected by *Cj*+/UV− conditions. These indices decreased in infected plants compared to healthy control (*Cj*−/UV−). The decline in NDVI, a broad proxy for photosynthetic activity, and NDNI, associated with nitrogen content, observed in infected plants are consistent with previous reports. Indeed, plant pathogen-induced chlorosis and necrosis lead to significant reductions in NDVI [69,70] meanwhile the NDNI decrease may be related to pathogen-induced disruption of nitrogen metabolism. Similarly, the reduction in CRI, which is sensitive to carotenoid content, may indicate that pathogen-induced oxidative stress led to carotenoid degradation as suggested by Mahlein et al. [69].

The results suggest that UV-C may act as a mild elicitor, priming defensive pigment production to mitigate pathogen spread. This effect is consistent with relevant scientific literature showing that hermetic UV-C doses stimulate plant natural defenses through multiple mechanisms, including increased activity of defense enzymes (e.g., phenylalanine ammonia-lyase, chitinase, β-1,3-glucanase), accumulation of antimicrobial compounds (e.g., phytoalexins, phenolics, lettucenin), and activation of both jasmonate- and salicylate-dependent signaling pathways [21,29,65,66]. Notably, the perception of UV-C flashes appears to be mediated by UV RESISTANCE LOCUS 8 (UVR8), the photoreceptor typically associated with UV-B perception, which may explain the enhanced efficacy of ultra-short exposures in eliciting defense responses [71]. The systemic nature of these UV-C-induced defenses, observed even in non-exposed tissues, further supports the potential of this approach for large-scale turfgrass management. Collectively, these indices offer a nuanced picture of turfgrass physiological status under stress and support the use of hyperspectral data not only for detection but also for monitoring plant responses to combined management treatments.

5. Conclusions

This study provides promising evidence for integrating autonomous UV-C treatment and hyperspectral sensing in sustainable turfgrass management. The use of robotic platforms for pathogen suppression and high-resolution, non-destructive monitoring could reduce reliance on chemical fungicides and improve the precision of disease control strategies. However, several challenges remain. UV-C operational constraints (e.g., speed, irradiance, treatment timing) and the complexity of hyperspectral data processing require further refinement. Future research should explore how to optimize UV-C application regimes, improve system scalability, and enhance the robustness of hyperspectral models across diverse turfgrass genotypes, growth stages, and environmental conditions. To enhance the practical and innovative value of our work, a two-step approach for future research is proposed: (1) the quantitative estimation of disease severity using conventional assessment methods, spectral indices, and machine learning models, and (2) the experimental determination of UV radiation responses to define optimal doses and exposure durations according to disease severity. Future experiments will focus on defining and calibrating a disease severity scale based on standardized visual assessments (e.g., percentage of affected leaf area or ordinal disease ratings), while simultaneously acquiring spectral data to combine severity evaluations with both traditional indices and full-spectrum analyses. The next steps toward implementing UV-C applications in grassland management will include developing regression models for continuous estimation of disease severity, conducting UV dose–response experiments across predefined severity levels, and establishing operational guidelines to balance treatment efficacy, plant safety, and management

costs. Importantly, combining both technologies into a unified platform could allow for simultaneous treatment and monitoring—an innovation that would significantly advance the field of automated plant health management.

Author Contributions: Conceptualization, L.I., E.P., M.R. and M.V.; methodology, C.P., L.C. (Lorenzo Cotrozzi), L.P. and L.G.; software, L.P., L.C. (Lorenzo Cotrozzi) and C.P.; validation, E.P., L.C. (Lorenzo Cotrozzi) and S.M.; formal analysis, L.P., L.G. and C.P.; investigation, L.P., L.G., C.P. and S.M.L.; resources, L.I., M.R., C.S., L.C. (Lorenzo Cotrozzi) and T.F.; data curation, L.P., L.C. (Lorenzo Cotrozzi), L.G., C.P., M.F. and S.M.L.; writing—original draft preparation, L.P., L.G., C.P., L.C. (Lorenzo Cotrozzi) and S.M.L.; writing—review and editing, L.P., L.G., S.M.L., L.C. (Lisa Caturegli), S.M. and M.S.; visualization, L.I., E.P., M.F., M.S., T.F. and M.V.; supervision, L.I., M.S., E.P. and L.C. (Lorenzo Cotrozzi); project administration, L.I.; funding acquisition, L.I., M.R., E.P. and M.V. All authors have read and agreed to the published version of the manuscript.

Funding: This work is supported by the project "Digitization of horticultural crops as a means to increase their sustainability" (DIGIORT, 488 PRA_2022_55) founded by the University of Pisa.

Data Availability Statement: Data are contained within the article.

Acknowledgments: This paper and related research was conducted during and with the support of the Italian national inter-university PhD course in Sustainable Development and Climate change. This publication was produced while attending the PhD program in PhD in Sustainable Development And Climate Change at the University School for Advanced Studies IUSS Pavia, Cycle XXXVIII, with the support of a scholarship financed by the Ministerial Decree no. 351 of 9 April 2022, based on the NRRP—funded by the European Union—NextGenerationEU—Mission 4 "Education and Research", Component 1 "Enhancement of the offer of educational services: from nurseries to universities"—Investment 4.1 "Extension of the number of research doctorates and innovative doctorates for public administration and cultural. The authors would also like to acknowledge the technicians of DAFE, Lorenzo Greci and Romano Zurrida, as well as the student Gabriele Tovani, for their technical support during the field trial.

Conflicts of Interest: The authors declare no conflicts of interest.

References

1. Goodman, D.M.; Burpee, L.L. Biological Control of Dollar Spot Disease of Creeping Bentgrass. *Phytopathology* **1991**, *81*, 1438–1446. [CrossRef]
2. Sapkota, S.; Catching, K.E.; Raymer, P.L.; Martinez-Espinoza, A.D.; Bahri, B.A. New Approaches to an Old Problem: Dollar Spot of Turfgrass. *Phytopathology* **2022**, *112*, 469–480. [CrossRef]
3. Mitkowski, N.A.; Colucci, S. The Identification of a Limited Number of Vegetative Compatibility Groups within Isolates of *Sclerotinia homoeocarpa* Infecting *Poa* spp. and *Agrostis palustris* from Temperate Climates. *J. Phytopathol.* **2006**, *154*, 500–503. [CrossRef]
4. Salgado-Salazar, C.; Beirn, L.A.; Ismaiel, A.; Boehm, M.J.; Carbone, I.; Putman, A.I.; Tredway, L.P.; Clarke, B.B.; Crouch, J.A. Clarireedia: A New Fungal Genus Comprising Four Pathogenic Species Responsible for Dollar Spot Disease of Turfgrass. *Fungal Biol.* **2018**, *122*, 761–773. [CrossRef] [PubMed]
5. Bennett, F.T. Dollar Spot Disease of Turf and Its Causal Organism, *Sclerotinia homoeocarpa* n. sp. *Ann. Appl. Biol.* **1937**, *24*, 236–257. [CrossRef]
6. Walsh, B.; Ikeda, S.S.; Boland, G.J. Biology and Management of Dollar Spot (*Sclerotinia homoeocarpa*); an Important Disease of Turfgrass. *HortScience* **1999**, *34*, 13–21. [CrossRef]
7. Tomaso-Peterson, M. A Demonstration Trial of Biofungicides with Efficacy for Controlling Dollar Spot in Turfgrasses. *Mississippi State Univ.* **2006**, *23*, 1–5.
8. Torsiello, J. Million Dollar Question. Golf Course Industry. 2015. Available online: https://www.golfcourseindustry.com/article/gci0315-dollar-spot-disease-control/ (accessed on 6 September 2025).
9. Bekken, M.A.H.; Soldat, D.J.; Koch, P.L.; Schimenti, C.S.; Rossi, F.S.; Aamlid, T.S.; Hesselsøe, K.J.; Peterson, T.K.; Straw, C.M.; Unruh, J.B.; et al. Analyzing Golf Course Pesticide Risk across the US and Europe—The Importance of Regulatory Environment. *Sci. Total Environ.* **2023**, *874*, 162498. [CrossRef]
10. Vargas, J.M. *Management of Turfgrass Diseases*, 3rd ed.; John Wiley & Sons: Hoboken, NJ, USA, 2005.

11. Steketee, C.J.; Martinez-Espinoza, A.D.; Harris-Shultz, K.R.; Henry, G.M.; Raymer, P.L. Evaluation of Seashore Paspalum Germplasm for Resistance to Dollar Spot. *Int. Turfgrass Soc. Res. J.* **2017**, *13*, 175–184. [CrossRef]
12. Sang, H.; Hulvey, J.; Popko, J.T.; Lopes, J.; Swaminathan, A.; Chang, T.; Jung, G. A Pleiotropic Drug Resistance Transporter Is Involved in Reduced Sensitivity to Multiple Fungicide Classes in *Sclerotinia homoeocarpa* (F.T. Bennett). *Mol. Plant Pathol.* **2015**, *16*, 251–261. [CrossRef]
13. Hu, J.; Yang, J.; Li, J.; Ma, Z.; Yao, W.; Ren, H.; Zhang, F.; Yang, G.; Sun, X.; Xiao, Y. Sensitivity of *Sclerotinia homoeocarpa* from Turfgrass to Thiophanate-Methyl, Iprodione and Propiconazole. *Chin. J. Pestic. Sci.* **2017**, *19*, 694–700.
14. Popko, J.T.; Sang, H.; Lee, J.; Yamada, T.; Hoshino, Y.; Jung, G. Resistance of *Sclerotinia homoeocarpa* Field Isolates to Succinate Dehydrogenase Inhibitor Fungicides. *Plant Dis.* **2018**, *102*, 2625–2631. [CrossRef]
15. Urban, L.; Charles, F.; De Miranda, M.R.A.; Aarrouf, J. Understanding the Physiological Effects of UV-C Light and Exploiting Its Agronomic Potential before and after Harvest. *Plant Physiol. Biochem.* **2016**, *105*, 1–11. [CrossRef] [PubMed]
16. De Oliveira, I.R.; Crizel, G.R.; Severo, J.; Renard, C.M.G.C.; Chaves, F.C.; Rombaldi, C.V. Preharvest UV-C Radiation Influences Physiological, Biochemical, and Transcriptional Changes in Strawberry cv. *Camarosa. Plant Physiol. Biochem.* **2016**, *108*, 391–399. [CrossRef] [PubMed]
17. Severo, J.; De Oliveira, I.R.; Bott, R.; Le Bourvellec, C.; Renard, C.M.G.C.; Page, D.; Chaves, F.C.; Rombaldi, C.V. Preharvest UV-C Radiation Impacts Strawberry Metabolite Content and Volatile Organic Compound Production. *LWT—Food Sci. Technol.* **2017**, *85*, 390–393. [CrossRef]
18. Xu, Y.; Charles, M.T.; Luo, Z.; Mimee, B.; Tong, Z.; Véronneau, P.; Roussel, D.; Rolland, D. Ultraviolet-C Priming of Strawberry Leaves against Subsequent Mycosphaerella fragariae Infection Involves the Action of Reactive Oxygen Species, Plant Hormones, and Terpenes. *Plant Cell Environ.* **2019**, *42*, 815–831. [CrossRef]
19. Zhang, W.; Jiang, H.; Cao, J.; Jiang, W. UV-C Treatment Controls Brown Rot in Postharvest Nectarine by Regulating ROS Metabolism and Anthocyanin Synthesis. *Postharvest Biol. Technol.* **2021**, *180*, 111613. [CrossRef]
20. Han, S.; Cai, H.; Yu, H.; Yu, Z.; Wu, Y. Targeted Metabolomic and Transcriptomic Reveal the Regulation of UV–C on Phenolics Biosynthesis of Peach Fruit during Storage. *LWT* **2023**, *190*, 115573. [CrossRef]
21. Vanhaelewyn, L.; Van Der Straeten, D.; De Coninck, B.; Vandenbussche, F. Ultraviolet Radiation from a Plant Perspective: The Plant-Microorganism Context. *Front. Plant Sci.* **2020**, *11*, 597642. [CrossRef]
22. Prämaßing, W. Effects of UV-C Radiation and Suståne Slow-Release Fertilzer on Turfgrass Diseases on Golf Greens. In Proceedings of the Symposium Sustainable Golf Courses: Integrated Turf Management, Sigtuna, Sweden, 18–19 September 2023.
23. Saga Robotics Grapevine—Thorvald. Available online: https://sagarobotics.com/crops/grapevine/ (accessed on 15 November 2024).
24. Gadoury, D.M.; Sapkota, S.; Cadle-Davidson, L.; Underhill, A.; McCann, T.; Gold, K.M.; Gambhir, N.; Combs, D.B.; Nyrop, J.P. Use of Germicidal UV Light to Suppress Grapevine Diseases and Arthropod Pests. *BIO Web Conf.* **2022**, *50*, 01002. [CrossRef]
25. Grossi, N.; Fontanelli, M.; Garramone, E.; Peruzzi, A.; Raffaelli, M.; Pirchio, M.; Martelloni, L.; Frasconi, C.; Caturegli, L.; Gaetani, M.; et al. Autonomous Mower Saves Energy and Improves Quality of Tall Fescue Lawn. *HortTechnology* **2016**, *26*, 825–830. [CrossRef]
26. Fontanelli, M.; Carlomagno, P.; Gagliardi, L.; Frasconi, C.; Raffaelli, M.; Peruzzi, A. Measuring Trampling in Autonomous Mowers with Systematic Trajectories: Comparison with the Ordinary Random Patterns. In Proceedings of the 2024 IEEE International Conference on Metrology for Agriculture and Forestry (MetroAgriFor), Padova, Italy, 29–31 October 2024.
27. SGL. Sustainable Fungal Disease Treatment UVC180. Available online: https://sglsystem.com/products/sustainable-grass-disease-management/the-uvc180/ (accessed on 10 April 2024).
28. UVBOOSTING. Helios Gazon: Technology for an Enhanced Turfgrass Protection. Available online: https://uvboosting.com/helios-gazon/?lang=en (accessed on 15 April 2025).
29. Urban, L.; Chabane Sari, D.; Orsal, B.; Lopes, M.; Miranda, R.; Aarrouf, J. UV-C Light and Pulsed Light as Alternatives to Chemical and Biological Elicitors for Stimulating Plant Natural Defenses against Fungal Diseases. *Sci. Hortic.* **2018**, *235*, 452–459. [CrossRef]
30. Urban, L.; Aarrouf, J.; Chabane Sari, D.; Orsal, B. Method for Stimulating the Resistance of Plants to Biotic Stress by UV Radiation Exposure. U.S. Patent 10,806,096, 20 October 2020.
31. Aarrouf, J.; Urban, L. Flashes of UV-C Light: An Innovative Method for Stimulating Plant Defences. *PLoS ONE* **2020**, *15*, e0235918. [CrossRef] [PubMed]
32. Mahlein, A.-K.; Kuska, M.T.; Behmann, J.; Polder, G.; Walter, A. Hyperspectral Sensors and Imaging Technologies in Phytopathology: State of the Art. *Annu. Rev. Phytopathol.* **2018**, *56*, 535–558. [CrossRef] [PubMed]
33. Cotrozzi, L. Spectroscopic Detection of Forest Diseases: A Review (1970–2020). *J. For. Res.* **2022**, *33*, 21–38. [CrossRef]
34. Ustin, S.L.; Jacquemoud, S. How the Optical Properties of Leaves Modify the Absorption and Scattering of Energy and Enhance Leaf Functionality. In *Remote Sensing of Plant Biodiversity*; Cavender-Bares, J., Gamon, J.A., Townsend, P.A., Eds.; SpringerOpen: Heidelberg, Germany, 2020; pp. 349–384.

35. Cotrozzi, L.; Couture, J.J. Hyperspectral Assessment of Plant Responses to Multi-Stress Environments: Prospects for Managing Protected Agrosystems. *Plants People Planet* **2020**, *2*, 244–258. [CrossRef]
36. Wang, Z.; Féret, J.-B.; Liu, N.; Sun, Z.; Yang, L.; Geng, S.; Zhang, H.; Chlus, A.; Kruger, E.L.; Townsend, P.A. Generality of Leaf Spectroscopic Models for Predicting Key Foliar Functional Traits across Continents: A Comparison between Physically- and Empirically-Based Approaches. *Remote Sens. Environ.* **2023**, *293*, 113614. [CrossRef]
37. Santin, M.; Caturegli, L.; Gagliardi, L.; Luglio, S.M.; Magni, S.; Pellegrini, E.; Pisuttu, C.; Raffaelli, M.; Volterrani, M.; Incrocci, L. Innovative Techniques for Managing Dollar Spot in Warm- and Cool-Season Turfgrasses: The Case of UV-B and UV-C Irradiations. *Agriculture* **2025**, *15*, 784. [CrossRef]
38. ISPRA—Istituto Superiore per la Protezione e la Ricerca Ambientale Rapporti 343/2021. Available online: https://www.isprambiente.gov.it/files2021/pubblicazioni/rapporti/r343-2021.pdf (accessed on 6 September 2025).
39. Valøen, L.O.; Shoesmith, M.I. The Effect of PHEV and HEV Duty Cycles on Battery and Battery Pack Performance. In Proceedings of the PHEV 2007 Conference: Where the Grid Meets the Road, Winnipeg, MB, Canada, 1 November 2007; p. 9.
40. May, G.J.; Davidson, A.; Monahov, B. Lead Batteries for Utility Energy Storage: A Review. *J. Energy Storage* **2018**, *15*, 145–157. [CrossRef]
41. Anderson, M.J. A New Method for Non-parametric Multivariate Analysis of Variance. *Austral Ecol.* **2001**, *26*, 32–46.
42. Dixon, P. VEGAN, a Package of R Functions for Community Ecology. *J. Veg. Sci.* **2003**, *14*, 927–930. [CrossRef]
43. Chevallier, S.; Bertrand, D.; Kohler, A.; Courcoux, P. Application of PLS-DA in Multivariate Image Analysis. *J. Chemom.* **2006**, *20*, 221–229. [CrossRef]
44. Kuhn, M. Building Predictive Models in R Using the Caret Package. *J. Stat. Soft.* **2008**, *28*, 1–26. [CrossRef]
45. Gamon, J.A.; Field, C.B.; Goulden, M.L.; Griffin, K.L.; Hartley, A.E.; Joel, G.; Penuelas, J.; Valentini, R. Relationships Between NDVI, Canopy Structure, and Photosynthesis in Three Californian Vegetation Types. *Ecol. Appl.* **1995**, *5*, 28–41. [CrossRef]
46. Gao, B. NDWI—A Normalized Difference Water Index for Remote Sensing of Vegetation Liquid Water from Space. *Remote Sens. Environ.* **1996**, *58*, 257–266. [CrossRef]
47. Gitelson, A.; Merzlyak, M.N. Quantitative Estimation of Chlorophyll-a Using Reflectance Spectra: Experiments with Autumn Chestnut and Maple Leaves. *J. Photochem. Photobiol. B Biol.* **1994**, *22*, 247–252. [CrossRef]
48. Gitelson, A.A.; Kaufman, Y.J.; Stark, R.; Rundquist, D. Novel Algorithms for Remote Estimation of Vegetation Fraction. *Remote Sens. Environ.* **2002**, *80*, 76–87. [CrossRef]
49. Gitelson, A.A.; Merzlyak, M.N.; Chivkunova, O.B. Optical Properties and Nondestructive Estimation of Anthocyanin Content in Plant Leaves. *Photochem. Photobiol.* **2001**, *74*, 38–45. [CrossRef]
50. Merzlyak, M.N.; Gitelson, A.A.; Chivkunova, O.B.; Rakitin, V.Y. Non-Destructive Optical Detection of Pigment Changes during Leaf Senescence and Fruit Ripening. *Physiol. Plant.* **1999**, *106*, 135–141. [CrossRef]
51. Serrano, L.; Peñuelas, J.; Ustin, S.L. Remote Sensing of Nitrogen and Lignin in Mediterranean Vegetation from AVIRIS Data: Decomposing Biochemical from Structural Signals. *Remote Sens. Environ.* **2002**, *81*, 355–364. [CrossRef]
52. Winkler, J.; Pasternak, G.; Sas, W.; Hurajová, E.; Koda, E.; Vaverková, M.D. Nature-Based Management of Lawns—Enhancing Biodiversity in Urban Green Infrastructure. *Appl. Sci.* **2024**, *14*, 1705. [CrossRef]
53. Janisiewicz, W.J.; Takeda, F.; Nichols, B.; Glenn, D.M.; Jurick Ii, W.M.; Camp, M.J. Use of Low-Dose UV-C Irradiation to Control Powdery Mildew Caused by Podosphaera Aphanis on Strawberry Plants. *Can. J. Plant Pathol.* **2016**, *38*, 430–439. [CrossRef]
54. Cote, S.; Rodoni, L.; Miceli, E.; Concellón, A.; Civello, P.M.; Vicente, A.R. Effect of Radiation Intensity on the Outcome of Postharvest UV-C Treatments. *Postharvest Biol. Technol.* **2013**, *83*, 83–89. [CrossRef]
55. Forges, M.; Bardin, M.; Urban, L.; Aarrouf, J.; Charles, F. Impact of UV-C Radiation Applied during Plant Growth on Pre- and Postharvest Disease Sensitivity and Fruit Quality of Strawberry. *Plant Dis.* **2020**, *104*, 3239–3247. [CrossRef]
56. Marquenie, D.; Lammertyn, J.; Geeraerd, A.H.; Soontjens, C.; Van Impe, J.F.; Nicolaı¨, B.M.; Michiels, C.W. Inactivation of Conidia of Botrytis Cinerea and Monilinia Fructigena Using UV-C and Heat Treatment. *Int. J. Food Microbiol.* **2002**, *74*, 27–35. [CrossRef]
57. Scolaro, E.; Beligoj, M.; Estevez, M.P.; Alberti, L.; Renzi, M.; Mattetti, M. Electrification of Agricultural Machinery: A Review. *IEEE Access* **2021**, *9*, 164520–164541. [CrossRef]
58. Luglio, S.M.; Frasconi, C.; Gagliardi, L.; Raffaelli, M.; Peruzzi, A.; Volterrani, M.; Magni, S.; Fontanelli, M. Analysis of Football Pitch Performances Based on Different Cutting Systems: From Visual Evaluation to YOLOv8. *Agronomy* **2024**, *14*, 2645. [CrossRef]
59. Gagliardi, L.; Sportelli, M.; Frasconi, C.; Pirchio, M.; Peruzzi, A.; Raffaelli, M.; Fontanelli, M. Evaluation of Autonomous Mowers Weed Control Effect in Globe Artichoke Field. *Appl. Sci.* **2021**, *11*, 11658. [CrossRef]
60. Ledermann, L.; Daouda, S.; Gouttesoulard, C.; Aarrouf, J.; Urban, L. Flashes of UV-C Light Stimulate Defenses of *Vitis vinifera* L. 'Chardonnay' Against *Erysiphe necator* in Greenhouse and Vineyard Conditions. *Plant Dis.* **2021**, *105*, 2106–2113. [CrossRef]
61. Badzmierowski, M.J.; McCall, D.S.; Evanylo, G. Using Hyperspectral and Multispectral Indices to Detect Water Stress for an Urban Turfgrass System. *Agronomy* **2019**, *9*, 439. [CrossRef]
62. Cushnahan, T.A.; Grafton, M.C.E.; Pearson, D.; Ramilan, T. Hyperspectral Data Can Differentiate Species and Cultivars of C3 and C4 Turf Despite Measurable Diurnal Variation. *Remote Sens.* **2024**, *16*, 3142. [CrossRef]

63. Kitchin, E.C.A.; Sneed, H.J.; McCall, D.S. Leveraging Deep Learning for Dollar Spot Detection and Quantification in Turfgrass. *Crop Sci.* **2025**, *65*, e21329. [CrossRef]
64. Horvath, B.J.; Vargas, J.M. Analysis of Dollar Spot Disease Severity Using Digital Image Analysis. *Int. Turfgrass Soc. Res. J.* **2005**, *10*, 196–201.
65. Loconsole, D.; Santamaria, P. UV Lighting in Horticulture: A Sustainable Tool for Improving Production Quality and Food Safety. *Horticulturae* **2021**, *7*, 9. [CrossRef]
66. Vàsquez, H.; Ouhibi, C.; Forges, M.; Lizzi, Y.; Urban, L.; Aarrouf, J. Hormetic Doses of UV-C Light Decrease the Susceptibility of Tomato Plants to Botrytis Cinerea Infection. *J. Phytopathol.* **2020**, *168*, 524–532. [CrossRef]
67. Nicolas, O.; Charles, M.; Chabot, D.; Aarrouf, J.; Jenni, S.; Toussaint, V.; Beaulieu, C. Preliminary Evaluation of the Impact of Preharvest UV-C on Lettuce: Potential for the Control of Xanthomonas campestris. *Acta Hortic.* **2020**, *1271*, 387–394. [CrossRef]
68. Pons, C.; Mas-Normand, L.; Chevallier, O.; Aarrouf, J.; Urban, L.; Lugan, R. Priming for Drought Resistance: UV-C Flashes Triggered Pipecolate Accumulation and Dehydration Avoidance in *Capsicum chinense* Jacq. but Induced No Growth or Metabolic Costs. *Environ. Exp. Bot.* **2024**, *226*, 105873. [CrossRef]
69. Mahlein, A.-K.; Oerke, E.-C.; Steiner, U.; Dehne, H.-W. Recent Advances in Sensing Plant Diseases for Precision Crop Protection. *Eur. J. Plant Pathol.* **2012**, *133*, 197–209. [CrossRef]
70. Bauriegel, E.; Herppich, W.B. Hyperspectral and Chlorophyll Fluorescence Imaging for Early Detection of Plant Diseases, with Special Reference to *Fusarium* spec. Infections on Wheat. *Agronomy* **2014**, *4*, 32–57. [CrossRef]
71. Aarrouf, J.; Hdech, D.B.; Diot, A.; Bornard, I.; Félicie, L.; Urban, L. Flashes of UV-C Light Are Perceived by UVR8, the Photoreceptor of UV-B Light. *J. Plant Sci. Phytopathol.* **2022**, *6*, 151–153. [CrossRef]

Disclaimer/Publisher's Note: The statements, opinions and data contained in all publications are solely those of the individual author(s) and contributor(s) and not of MDPI and/or the editor(s). MDPI and/or the editor(s) disclaim responsibility for any injury to people or property resulting from any ideas, methods, instructions or products referred to in the content.